Available online at www.sciencedirect.com
SCIENCE DIRECT
ELSEVIER
Journal of Crystal Growth 289 (2006) 502–505
JOURNAL OF CRYSTAL GROWTH
www.elsevier.com/locate/jcrysgro

MBE growth and structural and magnetic properties of $(In_{1-y}Al_y)_{1-x}Mn_xAs$-diluted magnetic semiconductors

W.N. Lee[a,*], Y.F. Chen[b], J.H. Huang[b], X.J. Guo[c], C.T. Kuo[a], H.C. Ku[d]

[a]*Department of Materials Science & Engineering, National Chiao Tung University, Hsinchu 300, Taiwan*
[b]*Department of Materials Science & Engineering, Materials Science Center, National Tsing Hua University, Hsinchu 300, Taiwan*
[c]*Institute of Physics, Academia Sinica, Taipei 11529, Taiwan*
[d]*Department of Physics, National Tsing Hua University, Hsinchu 300, Taiwan*

Received 27 February 2005; received in revised form 1 November 2005; accepted 14 December 2005
Available online 31 January 2006
Communicated by S. Hiyamizu

Abstract

A series of quaternary-diluted magnetic semiconductors, $(In_{1-y}Al_y)_{1-x}Mn_xAs$, have been successfully grown on InP substrates by low-temperature molecular beam epitaxy. The $(In_{0.52}Al_{0.48})_{1-x}Mn_xAs$ with $x \leqslant 0.11$ were grown on a nearly lattice-matched $In_{0.52}Al_{0.48}As$ buffer, while the $(In_{1-y}Al_y)_{1-x}Mn_xAs$ with a higher Mn content of $0.11 < x \leqslant 0.18$ were grown on a graded 3-layer $In_{1-y}Al_yAs$ buffer structure. The results of transmission electron microscopy and double-crystal X-ray diffraction reveal that all $(In_{1-y}Al_y)_{1-x}Mn_xAs$ epilayers are single crystal with zincblende structure, and the lattice constant increases with increasing the Mn content. The magnetic measurements show that the $(In_{1-y}Al_y)_{1-x}Mn_xAs$ semiconductors exhibit a paramagnetic-like state for $x \leqslant 0.05$ while a ferromagnetic state for $x > 0.05$, and the Curie temperature of ferromagnetic $(In_{1-y}Al_y)_{1-x}Mn_xAs$ increases with increasing Mn content.

PACS: 75.70.Ak; 81.15.Hi; 81.05.Zx; 73.61.Ey

Keywords: A3. MBE; B1. (In; Al; Mn) As; B2. Diluted ferromagnetic semiconductor

1. Introduction

Hole-mediated III–V-diluted magnetic semiconductors (DMS) [1–6] and DMS-based heterostructures [7–14] have been extensively studied to explore spin-dependent phenomena and properties of spintronic devices. Since the magnetism in III–V DMS is sensitive to both electronic and less understood structural properties of the metastable alloy, searching for new DMS becomes significant. Quaternary DMS, such as (In, Ga, Mn)As, grown on InP substrates are easier to adjust the bandgap energy, easy magnetization axis, and band structure by changing the indium content in comparison with ternary DMS. Recently, several groups have demonstrated the growth of quaternary $(In, Ga)_{1-x}Mn_xAs$ DMS on InP substrates [5,6,15,16] with Curie temperatures of 100–130 K. The quaternary $(In, Al)_{1-x}Mn_xAs$ DMS offers the possibility of fabricating complex heterostructures with engineered properties, combining magnetic layers having a large variety of electronic, optical, and spintronic properties in InP-based devices. In this article, we report the growth, crystalline structure, and magnetic properties of a series of $(In_{1-y}Al_y)_{1-x}Mn_xAs$ grown on InP substrates with Mn content of up to 0.18.

2. Experimental procedure

The samples used in this study were grown on (0 0 1) semi-insulating InP substrates by a Varian Modular

*Corresponding author. Materials Science Center, National Tsing Hua University, Hsinchu 300, Taiwan. Tel.: +886 35715131x5385; fax: +886 35713113.
E-mail addresses: wnlee@mx.nthu.edu.tw (W.N. Lee), jihhuang@mx.nthu.edu.tw (J.H. Huang).

0022-0248/$ - see front matter © 2006 Elsevier B.V. All rights reserved.
doi:10.1016/j.jcrysgro.2005.12.085

GEN-II MBE system with a growth rate of 0.3 μm/h and a V/III beam equivalent pressure (BEP) ratio of 20. Following native oxide desorption, a 100-nm $In_{0.52}Al_{0.48}As$ or a graded 3-layer $In_{1-y}Al_yAs$ buffer structure of 200-nm thick was grown at 460 °C. Growth was then interrupted and the substrate temperature was lowered to 200–230 °C. Finally, a 50 or 100 nm $(In_{1-y}Al_y)_{1-x}Mn_xAs$ epilayer of interest was grown. Since the $(In_{1-y}Al_y)_{1-x}Mn_xAs$ epilayers have larger lattice constants than the InP substrate, here we have employed different (In, Al)As buffer layer structures, in order to avoid the misfit-induced dislocation and to obtain a smooth starting surface for the growth of $(In_{1-y}Al_y)_{1-x}Mn_xAs$ epilayers. In this work, five samples with the $(In_{1-y}Al_y)_{1-x}Mn_xAs$ epilayers of different Mn contents ($x = 0.05$–0.18) have been successfully grown, and are denoted as A to E, respectively. The values of x and y and the thickness of the $(In_{1-y}Al_y)_{1-x}Mn_xAs$ epilayer and the corresponding buffer layer structure for the samples are given in Table 1. The surface reconstruction of the samples during growth was monitored in situ with the reflection high-energy electron diffraction (RHEED). Basically, a (2×4) RHEED pattern was observed during the growth of high-temperature (In, Al)As buffer layers, while it changed to (1×1) or (1×2) during and after the growth of (In, Al, Mn)As layer, implying a two-dimensional growth mode. Had the Mn flux or the substrate temperature been too high, a complicated RHEED pattern would have appeared, implying the formation of a second phase on the sample surface [17].

After growth, all $(In_{1-y}Al_y)_{1-x}Mn_xAs$ samples were cleaved into pieces for various characterizations. The Mn concentrations were determined by a calibration curve based on the electron microprobe analysis (EMPA). The crystalline structures were examined by double-crystal X-ray diffraction (DXRD) and transmission electron microscopy JEOL JEM-2010 (TEM). Cross-sectional samples parallel to (1 1 0) plane were prepared conventionally by mechanical thinning and Ar-ion milling for TEM observation. Magnetic properties were measured by a Quantum Design MPMS2 superconducting quantum interference device (SQUID) magnetometer.

3. Results and discussion

In order to check the crystalline structure and growth quality of (In, Al, Mn)As epilayers, DXRD rocking curves in the vicinity of InP (0 0 4) reflections were collected. Fig. 1 selectively shows the DXRD rocking curves of samples A, B, and D. All curves clearly exhibit well-separated diffraction peaks corresponding to the (In, Al)As buffer structures and the (In, Al, Mn)As epilayers, indicating that all samples are tetragonal and coherently full strained to the InP substrate. To resolve the diffraction peaks of sample D, a control sample consisting of only the graded buffer structure as used for sample D has been also grown under otherwise the same growth conditions. As a result, the extra peak of each sample was identified to be due to the (0 0 4) Bragg reflection of the (In, Al, Mn)As epilayer. The peak separations between the (In, Al, Mn)As epilayers and the InP substrate were found to be −280, −370, and −828 arcsec for samples A, B, and D, respectively. This indicates that (In, Al, Mn)As epilayers have larger lattices than InP. Moreover, the lattice constant of the (In, Al, Mn)As epilayers increases with increasing Mn content x, which agrees with what have observed for most (In, Ga,

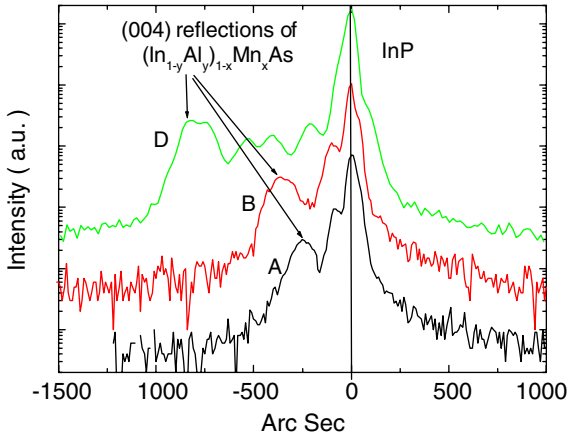

Fig. 1. The DXRD rocking curves of $(In_{1-y}Al_y)_{1-x}Mn_xAs$ samples A, B, and D.

Table 1
Layer structures of the $(In_{1-y}Al_y)_{1-x}Mn_xAs$ samples used in this study

Sample no.	Buffer layer structure	$(In_{1-y}Al_y)_{1-x}Mn_xAs$ epilayer
A	100-nm $In_{0.52}Al_{0.48}As$	100 nm; $y = 0.48$; $x = 0.05$
B	100-nm $In_{0.52}Al_{0.48}As$	100 nm; $y = 0.48$; $x = 0.08$
C	100-nm $In_{0.52}Al_{0.48}As$	100 nm; $y = 0.48$; $x = 0.11$
D	50-nm $In_{0.61}Al_{0.39}As$ 75-nm $In_{1-y}Al_yAs$; $0.39 < y < 0.45$ 75-nm $In_{0.55}Al_{0.45}As$	100 nm; $y = 0.39$; $x = 0.15$
E	50-nm $In_{0.63}Al_{0.37}As$ 75-nm $In_{1-y}Al_yAs$; $0.37 < y < 0.45$ 75-nm $In_{0.55}Al_{0.45}As$	50 nm; $y = 0.37$; $x = 0.18$

Mn)As [16] and (Ga, Mn)As [18] epilayers with appreciable Mn content. It has been noticed that the relationship between Mn content and lattice constant depends on many factors: the growth conditions, the size of the atoms that were substituted by Mn atoms, etc.

As already mentioned, appreciable Mn containing III–V alloys have a larger lattice than the supporting substrate, GaAs or InP, and the lattice constant in general increases linearly with increasing Mn content. However, the lattice-mismatch-induced strain associated with the enlarged (III, Mn)As lattice inhibit the growth of (III, Mn)As films beyond a certain thickness; i.e. the critical thickness. Therefore, the amount of Mn atoms that can be introduced to a III–V host should be lower than its chemical solubility if a high-quality (III, Mn)As film with fair thickness is needed. This problem can be overcome in principle by utilizing a buffer that is nearly lattice matched to the (III, Mn)As epilayer. Once the lattice-mismatch-induced compressive strain is greatly reduced, the III–V host can accommodate Mn atoms up to the chemical solubility limit; otherwise second phase or precipitation would form in the (III, Mn)As matrix to minimize the Gibbs free energy. In this study, we employed a graded buffer structure that was nearly lattice matched to the (In, Al, Mn)As films with high Mn content. As can be seen in Fig. 1, the peak separation between the $(In_{0.61}Al_{0.39})_{0.85}Mn_{0.15}As$ epilayer and the $In_{0.61}Al_{0.39}As$ buffer is only ~70 arcsec, indicating both layers are nearly lattice matched to each other. In contrast, the $(In_{0.61}Al_{0.39})_{0.85}Mn_{0.15}As$ is ~828 arcsec apart from the InP. Without this graded buffer, it was found that only ~10 nm $(In_{0.61}Al_{0.39})_{0.85}Mn_{0.15}As$ could be grown prior to the onset of island growth.

The cross-sectional high-resolution lattice image projected along the [1 1 0] zone of sample C is shown in Fig. 2a, which shows a high-quality interface between the $(In_{0.52}Al_{0.48})_{0.89}Mn_{0.11}As$ epilayer and the $In_{0.52}Al_{0.48}As$ buffer. Moreover, the image shows no trace of Moiré fringes, implying the films are free of structural defects, such as twins and/or precipitates [19]. The selected area diffraction pattern of the $(In_{0.52}Al_{0.48})_{0.89}Mn_{0.11}As$ layer shown in Fig. 2b further shows no extra diffractive spots. Therefore, from Fig. 2, it can be concluded that the $(In_{0.52}Al_{0.48})_{0.89}Mn_{0.11}As$ layer is of perfect single crystal with zinc-blende structure.

The magnetic field dependence of magnetization (M–H curves) of samples A, B, C, and D at 5 K are shown in Fig. 3. The samples were measured with in-plane magnetic field applied along the $[\bar{1}\,1\,0]$ direction, and the diamagnetic behavior of the InP substrate was carefully subtracted from the measured signals. All curves are not square like, which is a result of the magnetic anisotropy. Obviously, the $[\bar{1}\,1\,0]$ is not magnetic easy axis. Analogous to a detailed study on this respect has been given by Welp et al. [20], who investigated the evolution of magnetic anisotropy in a series of $Ga_{1-x}Mn_xAs$ films. Furthermore, it is noticed that the M–H curve of sample A can be perfectly fitted with a straight line, suggesting that the $(In_{0.52}Al_{0.48})_{0.95}Mn_{0.05}As$ exhibits a paramagnetic-like behavior at 5 K. In contrast, all other samples with $x > 0.05$ demonstrate ferromagnetic states at 5 K, as confirmed by their M–H curves.

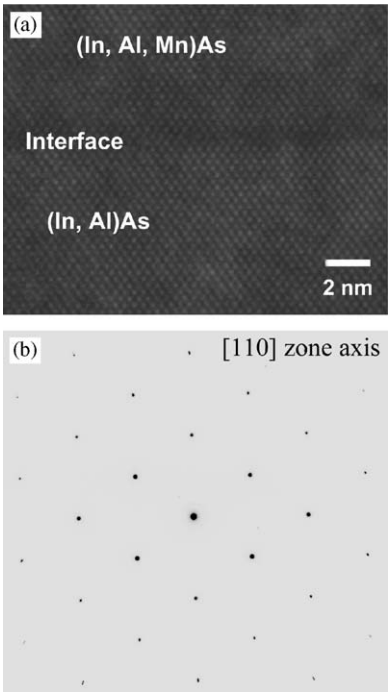

Fig. 2. (a) High-resolution lattice image of the $(In_{0.52}Al_{0.48})_{0.89}Mn_{0.11}As$/$In_{0.52}Al_{0.48}As$ interface region and (b) the selected area diffraction pattern of $(In_{0.52}Al_{0.48})_{0.89}Mn_{0.11}As$ layer along [1 1 0] zone axis.

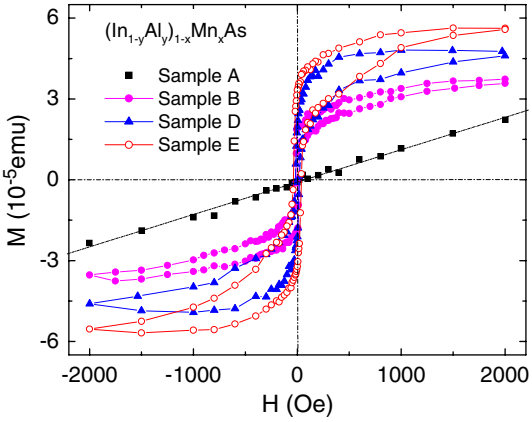

Fig. 3. The magnetic field dependence of magnetization for $(In_{1-y}Al_y)_{1-x}Mn_xAs$ samples A, B, D, and E with in-plane magnetic field applied along the $[\bar{1}\,1\,0]$ direction. The dash dot line is a linear fit of the M–H curve for sample A.

The temperature dependence of magnetization (M–T curve) for the ferromagnetic samples was measured with a small magnetic field of 100 Oe along the $[\bar{1}\,1\,0]$ direction. Fig. 4 shows the M–T curves of samples B, C, D, and E, from which the Curie temperature, T_C, of each sample is determined. The values of T_C for samples B, C, D, and E are found to be 20, 25, 30, and 40 K, respectively.

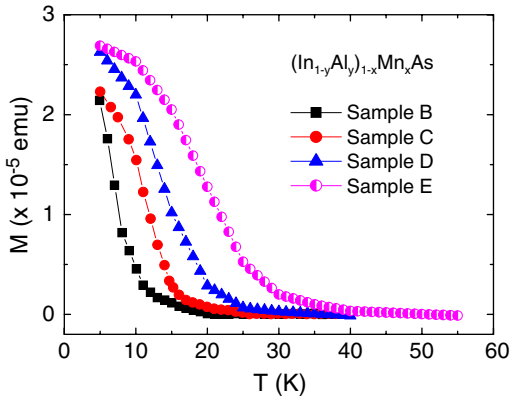

Fig. 4. The temperature dependence of magnetization for $(In_{1-y}Al_y)_{1-x}Mn_xAs$ samples B, C, D, and E in a small magnetic field ($H = 100$ Oe) applied along the $[\bar{1}\,1\,0]$ direction.

The increase of T_C with increasing Mn content is unambiguously a result as generally expected for III–V DMS materials.

4. Conclusion

In summary, we have successfully grown a series of quaternary DMS, $(In_{1-y}Al_y)_{1-x}Mn_xAs$ ($x \leqslant 0.18$), on InP substrates by low-temperature molecular beam epitaxy. The results of TEM and DXRD show that $(In_{1-y}Al_y)_{1-x}Mn_xAs$ epilayers are of single crystal with zinc-blende structure and the lattice constant increases with increasing Mn content, x. The results of magnetic measurements show that the $(In_{1-y}Al_y)_{1-x}Mn_xAs$ semiconductors exhibit a paramagnetic-like state for $x \leqslant 0.05$ but a ferromagnetic state for $x > 0.05$, and the Curie temperatures of ferromagnetic $(In_{1-y}Al_y)_{1-x}Mn_xAs$ increase with increasing Mn content.

Acknowledgments

This work was supported by the National Science Council, Republic of China, under Contract nos. NSC 92-2112-M-007-032 and NSC 92-2120-M-007-006.

References

[1] T. Dietl, H. Ohno, F. Matsukura, J. Cibert, D. Ferrand, Science 287 (2000) 1019.
[2] H. Munekata, H. Ohno, S. von Molnár, A. Segmüller, L.L. Chang, L. Esaki, Phys. Rev. Lett. 63 (1989) 1849.
[3] H. Ohno, A. Shen, F. Matsukura, A. Oiwa, A. Endo, S. Katsumoto, Y. Iye, Appl. Phys. Lett. 69 (1996) 363.
[4] A. van Esch, L. van Bockstal, J. de Boeck, G. Verbanck, et al., Phys. Rev. B 56 (1997) 13103.
[5] T. Slupinski, H. Munekata, A. Oiwa, Appl. Phys. Lett. 80 (2002) 1592.
[6] S. Ohya, H. Kobayashi, M. Tanaka, Appl. Phys. Lett. 83 (2003) 2175.
[7] H. Ohno, J. Magn. Magn. Mater. 272–276 (2004) 1.
[8] M. Tanaka, Y. Higo, Phys. Rev. Lett. 87 (2001) 026602.
[9] Y. Ohno, D.K. Young, B. Beschoten, F. Matsukura, H. Ohno, D.D. Awschalom, Nature 402 (1999) 790.
[10] E. Johnston-Halperin, D. Lofgreen, R.K. Kawakami, D.K. Young, L. Coldren, A.C. Gossard, D.D. Awschalom, Phys. Rev. B 65 (2002) 041306.
[11] H. Ohno, D. Chiba, F. Matsukura, T. Omiya, E. Abe, T. Dietl, Y. Ohno, K. Ohtani, Nature 408 (2000) 944.
[12] S. Koshihara, A. Oiwa, M. Hirasawa, S. Katsumoto, Y. Iye, C. Urano, H. Takagi, H. Munekata, Phys. Rev. Lett. 78 (1997) 4617.
[13] H. Boukari, P. Kossacki, M. Bertolini, D. Ferrand, J. Cibert, S. Tatarenko, A. Wasiela, J.A. Gaj, T. Dietl, Phys. Rev. Lett. 88 (2002) 207204.
[14] D. Chiba, M. Yamanouchi, F. Matsukura, H. Ohno, Science 301 (2003) 943.
[15] T. Slupinski, H. Munekata, A. Oiwa, J. Supercond. 16 (2003) 45.
[16] S. Ohya, H. Yamaguchi, M. Tanaka, J. Supercond. 16 (2003) 139.
[17] J.B. Park, K.H. Kim, K.J. Lee, D.J. Kim, H.J. Kim, Y.E. Ihm, J. Crystal Growth 273 (2005) 396.
[18] J. Sadowski, L.Z. Domagala, Phys. Rev. B 69 (2004) 075206.
[19] J.H. Huang, L.Z. Hsieh, X.J. Guo, Y.O. Su, Appl. Phys. Lett. 82 (2003) 3005.
[20] U. Welp, V.K. Vlasko-Vlasov, A. Menzel, H.D. You, X. Liu, J.K. Furdyna, T. Wojtowicz, Appl. Phys. Lett. 85 (2004) 260.